ELSEVIER

International Journal of Mass Spectrometry 209 (2001) 209–226

International Journal of Mass Spectrometry

www.elsevier.com/locate/ijms

A simulation study of coupled secular oscillations in nonlinear Paul trap mass spectrometers

S. Sevugarajan, A.G. Menon*

Department of Instrumentation, Indian Institute of Science, Bangalore −560012, India

Received 9 March 2001; accepted 14 July 2001

Abstract

This paper presents the results of a simulation study of coupled axial and radial secular motion in nonlinear Paul trap mass spectrometers. The nonlinearities included in the simulation are external excitation and hexapole and octopole field aberrations. The equations of motion have the form of an inhomogeneous-coupled Duffing oscillator with quadratic, cubic nonlinearities and periodic forcing function in the axial direction. The study used a numerical technique to probe the role of field inhomogeniety and external excitation in the appearance of coupled frequencies in axial and radial directions. The multiple scales perturbation technique was used to develop an analytical expression for frequency perturbation. It is seen that the strength of coupling can be characterized by the magnitude of the coefficient of the cross terms in the equations of motion and the appearance of coupled frequencies in each direction is a function of this coupling strength. Hexapole superposition affects in the coupling strength of only the axial direction and its influence in coupled oscillations is minimal. Octopole superposition plays the predominant role in the manifestation of coupled frequencies in both directions. In the presence of external excitation, a larger number of frequencies appear in the frequency spectrum because of the mixing of fundamental and harmonic frequencies in the axial and radial directions. In the presence of external excitation, the axial secular motion is amplitude and phase modulated, and results in a beat frequency corresponding to the difference between the perturbed axial frequency and the applied excitation frequency. (Int J Mass Spectrom 209 (2001) 209–226) © 2001 Elsevier Science B.V.

Keywords: Nonlinear traps; Perturbed secular frequency; Coupling; Coupling strength; Excitation; Beats; Beat frequency

1. Introduction

The Paul trap mass spectrometer consists of a three electrode mass analyzer with two end cap electrodes and one central ring electrode [1]. These electrodes are mechanically shaped [2] so that when an oscillating rf potential is applied between the ring and end cap electrodes, an essentially linear field is produced in the cavity. Fragment ions of an analyte gas, which are produced in or introduced into the central cavity, experience a trapping field and execute stable trajectories that are functions of trap geometry and experimental parameters [3].

The equations of motion of the trapped ion in an ideal Paul trap mass spectrometer are represented by the linear Mathieu equations [4,5] and their stability is governed by the two Mathieu parameters a and q. The motion of the ion in the axial and radial directions is decoupled, and consists of a large-amplitude secular motion superimposed by a micromotion with a frequency corresponding to the rf drive. At values of q

* Corresponding author. E-mail: agmenon@isu.iisc.ernet.in

PII S1387-3806(01)00501-2

less than 0.4, the amplitude of the micromotion can be considered negligible in comparison to the amplitude of the secular motion, and it is possible to use the pseudopotential well method to arrive at an expression for the parameter β_u as [6]

$$\beta_u = a_u + \left(\frac{q_u^2}{2}\right)^{1/2} \quad (1)$$

where the subscript u corresponds to the z and r direction. Eq. (1) is referred to as the Dehmelt or adiabatic approximation in literature [6]. The secular frequency, ω_{0u}, in ideal Paul traps in the two directions can be obtained from the expression

$$\omega_{0u} = \beta_u \Omega / 2 \quad (2)$$

In practical traps a variety of factors affect ion dynamics. These factors include geometric aberrations caused by holes in the end cap electrodes, truncation of electrodes to finite size, and improper machining [1], experimental constraints such as mechanical misalignment [7], damping caused by buffer gas [8,9], space charge [10–12], and externally applied (ac) supplementary voltage [13,14] in experiments such as resonant excitation [15,16] and broadband excitation [17]. The ion dynamics can be altered by mildly nonlinear fields and has been reported in mass spectrometry literature. Reports include observations of nonlinear resonances [18], perturbation of secular frequencies [19,20], appearance of harmonics in ion motion [21], and coupled secular oscillations [21–23].

The causes and consequences of field nonlinearities in Paul traps have received some theoretical attention. Franzen et al. have extensively investigated nonlinear resonances [18] and attribute them to a match between a large set of harmonics of secular frequency and a family of sidebands. Their analysis shows that condition necessary for nonlinear resonance could be estimated from a specific relationship of axial, radial, and rf frequencies [24]. Makarov [25] investigated the jump phenomenon associated with the Duffing equation [26,27] as a means to explain the high resolution obtained in resonance excitation experiments. Two recent papers report attempts to understand frequency perturbation in practical Paul traps [28,29]. Simulation studies of ion motion in nonlinear Paul traps include ion simulation program ISIS by Londry et al. [30], quadrupole resonance program SPQR by March et al. [31,32], and multiparticle simulation for studying ion-ion interaction as well as the and ion-neutral interaction proposed by Bui and Cooks [33].

One aspect of ion dynamics that has not yet received adequate attention is the coupled secular motion within the practical Paul trap. Some investigators provide evidence for such coupling in recent experimental studies. Vedel et al. [23] in their study of a stored ion cloud note the coupling of motion in radial and axial directions. The experiments involved mass selective destabilization of stored ions by sweeping the tickle frequency applied across end cap electrodes. Chu et al. [21] in their experiments of higher order motional resonances in ion clouds have also reported coupled oscillations. In addition to harmonic modes of axial secular frequency combining with harmonics of rf drive frequency, the appearance of radial and radial-axial coupled frequencies has been reported by them.

The need for studying coupled oscillation is particularly relevant in Paul traps. Such traps are widely used in a variety of experiments including the spectroscopy of charge clouds [34,35] and single ions [36,37] as well as in mass spectrometry [38]. In mass spectrometry, understanding of the ion dynamics associated with coupled secular oscillation is important especially with respect to experiments that use broadband detection of image current [20,39] for obtaining mass spectra of analyte samples. In these experiments, coupled oscillations will induce secular frequency perturbation resulting in problems with mass assignment. Besides, coupled oscillations are likely to cause phantom peaks of radial secular frequencies in broadband detection of image currents across end cap electrodes.

The motivation of the present paper is to understand the coupled oscillations associated with nonlinear practical Paul traps. Two types of nonlinearities, viz., field inhomogeniety and dipolar external excitation, have been considered. Field inhomogeniety will

be modeled as predominantly linear, with weak hexapole and octopole superpositions. External excitation will be introduced as a periodic forcing function in the axial direction with a frequency corresponding to the ideal axial secular frequency (secular frequency when there is no nonlinearity). The equations of motion in the axial and radial directions will be solved numerically to obtain the ion trajectories as well as to determine the frequency spectrum in axial and radial motions. A perturbation technique will be used to obtain an analytical expression for perturbed secular frequencies in axial and radial directions. The results of these simulations will be used to understand the role of nonlinearities in coupling axial and radial secular motions.

2. Equations of ion motion in nonlinear fields

The potential within a nonlinear ion trap is represented by superposing weak higher order terms on the pure quadrupolar potential. In an ideal quadrupolar trap, the potential distribution inside the trap has both spherical and rotational symmetry. If there are geometrical aberrations in the trap, a set of orthogonal functions are chosen in such a way that it has the same symmetry as the system for representing the higher order terms. Legendre polynomials are normally selected for expressing these nonlinearities [40,41].

If P_n is the Legendre polynomial of order n, then the potential distribution inside the trap in terms of spherical coordinates is given by

$$\phi\,(\rho,\,\theta,\,\varphi) = \phi_0 \sum_{n=0}^{\infty} A_n \frac{\rho^n}{r_0^n} P_n\,(\cos\theta) \tag{3}$$

where ρ is the position vector and ϕ_0 is a time dependent quantity and is given by

$$\phi_0 = U_0 + V_0 \cos\Omega t \tag{4}$$

and U_0 = magnitude of the dc potential, V_0 = 0-peak voltage of the rf potential, Ω = angular frequency of the rf potential, A_n = dimensionless weight factors for different terms, and r_0 = radius of the ring electrode.

The various terms corresponding to $n = 0, 1, 2, 3 \ldots$ etc. represent the multipole components of the potential.

In the present work, two higher order multipoles viz., hexapole and octopole corresponding to $n = 3$ and 4, are taken into account along with the quadrupole component for calculating the potential distribution inside the trap. Eq. (3) becomes simpler if we write the multipole components in terms of time dependent r and z cylindrical coordinates. The multipole component corresponding to $n = 2$–4 in terms of cylindrical coordinates can be written as follows [42]

$$P_2\,(\cos\theta) = \frac{2z^2 - r^2}{2\rho^2} \tag{5}$$

$$P_3\,(\cos\theta) = \frac{2z^3 - 3zr^2}{2\rho^3} \tag{6}$$

$$P_4\,(\cos\theta) = \frac{8z^4 - 24z^2r^2 + 3r^4}{8\rho^4} \tag{7}$$

where

$$\rho^2 = z^2 + r^2 \tag{8}$$

Expanding Eq. (3) by substituting Eqs. (4), (5), (6), and (7) we get the following final expression for the potential distribution inside the trap:

$$\phi\,(r,\,z,\,t) = \frac{A_2}{r_0^2}\,(U_0 + V_0\cos\Omega t) \cdot \left[z^2 - \frac{r^2}{2} + \frac{h}{r_0}\left(z^3 - \frac{3}{2}r^2 z\right) + \frac{f}{r_o^2} \cdot \left(z^4 - 3r^2z^2 + \frac{3}{8}r^4\right)\right] \tag{9}$$

where $h = A_3/A_2$ and $f = A_4/A_2$. Here A_2, A_3, and A_4 refer to the weight of the quadrupole, hexapole, and octopole superposition, respectively. The parameter f and h represent octopole and hexapole superposition relative to the quadrupole contribution.

In classical mechanics, the three-dimensional motion of an ion within a pseudopotential well [43] with excitation potential applied to the end cap electrode is given by

$$m\frac{d^2\rho}{dt^2} + e\,\nabla\,U_{eff}(r,z) = -e\,\nabla\,U_{exc} \tag{10}$$

where ρ is the ion position vector, e is the charge of electron, m is the mass of the ion. U_{eff} and U_{exc} are the effective potential inside the ion trap and the excitation potential applied to the end cap electrodes respectively and are given by

$$U_{eff}(r,z) = \frac{1}{2}\frac{e}{m}\left\langle \left| \int \nabla\,\phi dt \right|^2 \right\rangle \tag{11}$$

$$U_{exc}(r,z,t) = A_1 V_s \cos(\omega_z t)\left[\frac{z}{r_0}\right] \tag{12}$$

Here, A_1 is the weight of dipole superposition and can be calculated by the data given by Beaty [41], V_s is the amplitude of the excitation potential, and ω_z is the angular frequency of the dipolar excitation potential that is applied to the end cap electrodes.

When Eq. (11) is integrated under the assumption $V_0 >> U_0$, U_{eff} takes the form

$$U_{eff}(r,z) = \frac{1}{\lambda}(\omega_{0u}^2)\left(\frac{m}{e}\right)\left(\begin{array}{l} r^2 + \dfrac{9h^2r^2z^2}{r_0^2} + \dfrac{6hzr^2}{r_0} - \dfrac{12fz^2r^2}{r_0^2} - \dfrac{3fr^4}{r_0^2} + 4z^2 + \\ \dfrac{h^2}{r_0^2}\left(9z^4 - 9z^2r^2 + \dfrac{9r^4}{4}\right) + \dfrac{12h}{r_0}z^3 - \dfrac{6hzr^2}{r_0} + \dfrac{16f}{r_0^2}z^4 \end{array}\right) \tag{13}$$

where $\lambda = 8$ for z direction and $\lambda = 2$ for r direction and

$$\omega_{0u}^2 = \left(a_u + \frac{q_u^2}{2}\right)\frac{\Omega^2}{4} \tag{14}$$

with

$$a_z = -2a_r = -\frac{8eU}{mr_0^2\Omega^2} \tag{15}$$

$$q_z = -2q_r = \frac{4eV_0}{mr_0^2\Omega^2} \tag{16}$$

Substituting Eqs. (12) and (13) in Eq. (10), we get the following equation of ion motion in the axial direction

$$\frac{d^2z}{dt^2} + \omega_{0z}^2 z + \frac{9h}{2r_0}\omega_{0z}^2 z^2 + \left(8f + \frac{9h^2}{2}\right)\frac{\omega_{0z}^2 z^3}{r_0^2} + \left(\frac{9h^2}{4} - 3f\right)\frac{\omega_{0z}^2 z r^2}{r_0^2} = -F_s\cos(\omega_z t) \tag{17}$$

where

$$F_s = \frac{eA_1V_s}{mr_0} \tag{18}$$

In the radial (r) direction the equation of ion motion can be written as

$$\frac{d^2r}{dt^2} = \omega_{0r}^2 r - \left(6f\frac{9h^2}{2}\right)\frac{\omega_{0r}^2 r^3}{r_0^2} - \frac{12f\omega_{or}^2 r z^2}{r_0^2} = 0 \tag{19}$$

In Eq. (19) the right hand side is zero as there is no excitation potential applied in the radial direction. The equations of ion motion in axial and radial directions can now be rewritten in a simplified form as

$$\frac{d^2z}{dt^2} + \omega_{0z}^2 z + \alpha_2\omega_{0z}^2 z^2 + \alpha_3 z^3 - \alpha_4 z r^2 = -F_s\cos(\omega_z t) \tag{20}$$

$$\frac{d^2r}{dt^2} + \omega_{0r}^2 r - \alpha_5 r^3 - \alpha_6 r z^2 = 0 \tag{21}$$

where

$$\alpha_2 = \frac{9h\omega_{0z}^2}{2r_0} \tag{22}$$

$$\alpha_3 = \left(8f + \frac{9h^2}{2}\right)\frac{\omega_{0z}^2}{r_0^2} \tag{23}$$

$$\alpha_4 = c_z \frac{\omega_{0z}^2}{r_0^2} \tag{24}$$

$$\alpha_5 = \left(6f - \frac{9h^2}{2}\right)\frac{\omega_{0r}^2}{r_0^2} \tag{25}$$

$$\alpha_6 = c_r \frac{\omega_{0r}^2}{r_0^2} \tag{26}$$

$$c_z = \left(3f - \frac{9h^2}{4}\right) \tag{27}$$

$$c_r = 12f \tag{28}$$

Here c_z and c_r represents the coupling strength due to hexapole and octopole in the coefficient of cross terms (α_4 and α_6) in Eqs. (20) and (21).

It must be noted here that Eqs. (20) and (21) has been developed on the basic premise that the ions are oscillating in the trap within a pseudopotential well. Consequently, the results of the computations are valid for values of $q_z = 0.4$ up to which we can assume that the amplitude of micro motion is negligibly small. Within this limit, the calculation of secular frequencies using the Dehmelt approximation and the calculation of secular frequencies from β_u values from the continuous fraction [1,44] are accurate to about 3%.

The nonlinear system governed by Eqs. (20) and (21) represents the coupled ion dynamics in *z* and *r*directions. In these equations α_2, α_3, and α_4 are the coefficients of quadratic, cubic and cross terms respectively in the axial direction. In the *z* direction of motion, the right hand side represents the forcing term which is a function of excitation potential V_s applied to the end cap electrode. Similarly, in the *r* direction, α_5 and α_6 represent the coefficients of cubic and cross terms respectively in the radial direction. Since there is no external excitation applied in the *r* direction, there is no forcing term in the right hand side of the equation of ion motion.

The system of equations represented by Eqs. (20) and (21) is similar to those of nonlinear mechanical and physical systems with two degrees of freedom. Such systems have been discussed in mathematical literature extensively. Nayfeh and Zavodney [45] used similar equations for studying the responses of two internally coupled oscillators to harmonic excitation. Nayfeh and Nayfeh [46] analyzed the nonlinear interaction between two widely spaced modes subjected to external excitation to study the transfer of energy between a system of equations with quadratic and cubic nonlinearity. Coupled systems of equations containing linear and quadratic coupling terms have been used by Nayfeh et al. [47] in their study of the coupling of pitch and roll modes in ship motions. Similar coupled equations have also been proposed by Efstathiades [48] in his mathematical model of coupled motion in nonlinear vibration isolation systems. Yamamoto and Yasuda [49] have used coupled equations with the potential function having quadratic and cubic terms for studying internal resonance in nonlinear systems with two degrees of freedom. The system of equations represented by Eqs. (20) and (21) has also been used by Reynolds and Dowell [50] and Tseng and Dugundji [51] in their studies of nonlinear vibration of buckled beams. Tien et al. [52] used a similar system for investigating the nonlinear dynamics of a shallow arch under periodic excitation.

3. Methods of analysis

The equations of motion developed above have the form of an inhomogeneous coupled Duffing oscillator with quadratic and cubic nonlinearities with an external periodic forcing function in one direction. We have used two mathematical methods for investigating the axial and radial coupled ion motions. The first is a numerical technique to obtain the trajectories and frequency spectrum of ions. The second is an analytical method to study the role of field inhomogeniety and external excitation in perturbing the ion secular frequencies. The numerical technique has been adapted for obtaining the trajectories and frequency spectrum in coupled oscillations because analytical methods become intractable if a priori knowledge of coupled frequencies is unavailable. Frequency perturbation, on the other hand, is amenable to such analyses and it is possible to obtain expressions for

frequency perturbations caused by field inhomogeniety, external excitation, and coupling.

In the two mathematical methods we have used, there are two different frequencies in the forcing term in conformity with the practice reported in mathematical literature [45]. The numerical technique assumes that the excitation frequency corresponds to the ideal secular frequency, that is, secular frequency when there is no nonlinearity in the system. This ensures that the excitation frequency is different from the perturbed secular frequency. If the excitation frequency is kept the same as the perturbed frequency, the trajectory of the ions will become unbounded in the simulations. In the analytical method used for obtaining perturbed secular frequency, the frequency of the force term is assumed to be equal to the perturbed secular frequency. This assumption is required because in perturbation techniques, the frequency of the force term is evaluated to estimate perturbed frequencies.

4. Numerical simulation of ion trajectories

For simulating the coupled ion motion, we have used MATLAB's toolbox SIMULINK [53]. The 4^{th} order Runge-Kutta numerical integration algorithm is used for solving the equation of ion motion in z and r directions. Considering that the maximum secular frequencies that will be encountered in our studies will be around 62 kHz the step size is fixed at 1e-6, which satisfies the Nyquist criteria for avoiding frequency aliasing in the Fourier frequency spectrum. We obtained the Fourier spectrum from the fast Fourier transform (FFT) algorithm available in MATLAB. MATLAB uses a radix-2 FFT algorithm if the length of the sequence is a power of two, and a slower mixed-radix algorithm if it is not. In all our computations we have used a 4096 point FFT and plotted the first 2048 points to obtain the frequency information on the positive side of the frequency axis.

As an example, Eqs. (20) and (21) were numerically integrated for an operating point corresponding to an rf potential of $259.6V_{0-p}$ and a dc potential of 9.3 *V*. Here, the nonlinear conditions are kept at 1% hexapole and 5% octopole superposition. The magnitude of 5% octopole superposition is high in this simulation to provide a contrast to the 2.5% octopole superposition in subsequent simulations. It is also assumed that an external excitation of 300 mV is applied to the end cap electrodes. Figs. 1(a) and 1(b) show the unfiltered time trace of the ions in axial and radial directions, respectively. Following the method adopted by Nayfeh [45], Figs. 1(c) and 1(d) show the filtered fundamental secular frequency components in axial and radial directions, respectively. The fundamental component (Fig. 1(c), 1(d)) is filtered from the unfiltered [Figs. 1(a), 1(b)] ion motion by implementing an 8^{th} order Butterworth filter function in MATLAB.

5. Frequency perturbation

There are several mathematical techniques to estimate frequency perturbation in nonlinear systems. In earlier studies of axial secular frequency perturbation in nonlinear Paul traps [28,29] we had used the conventional as well as a modified Lindstedt-Poincare technique for investigating the perturbation in ion axial secular frequencies. The conventional Lindstedt–Poincare perturbation technique is useful when the system nonlinearity is assumed to have a weak nonlinear superposition. The modified Lindstedt-Poincare method was used when the strength of the nonlinearity was large. However, both these methods have involved algebra in the context of coupled equations of motion. A method widely used in mathematical literature for studying coupled systems is the multiple scales method. It was also found suitable for estimating perturbed frequencies in our applications and has therefore been used in the present investigations.

The computation of secular frequency perturbation in nonlinear systems that have a forcing term assumes that the frequency of the forcing term is equal to the perturbed secular frequency [54,55]. It is also assumed that the perturbed frequency is close to the natural frequency of the ideal systems (i.e. $\omega_z \cong \omega_{0z}$) and can be represented as

$$\omega_z = \omega_{0z} + \in^2 \sigma_z \tag{29}$$

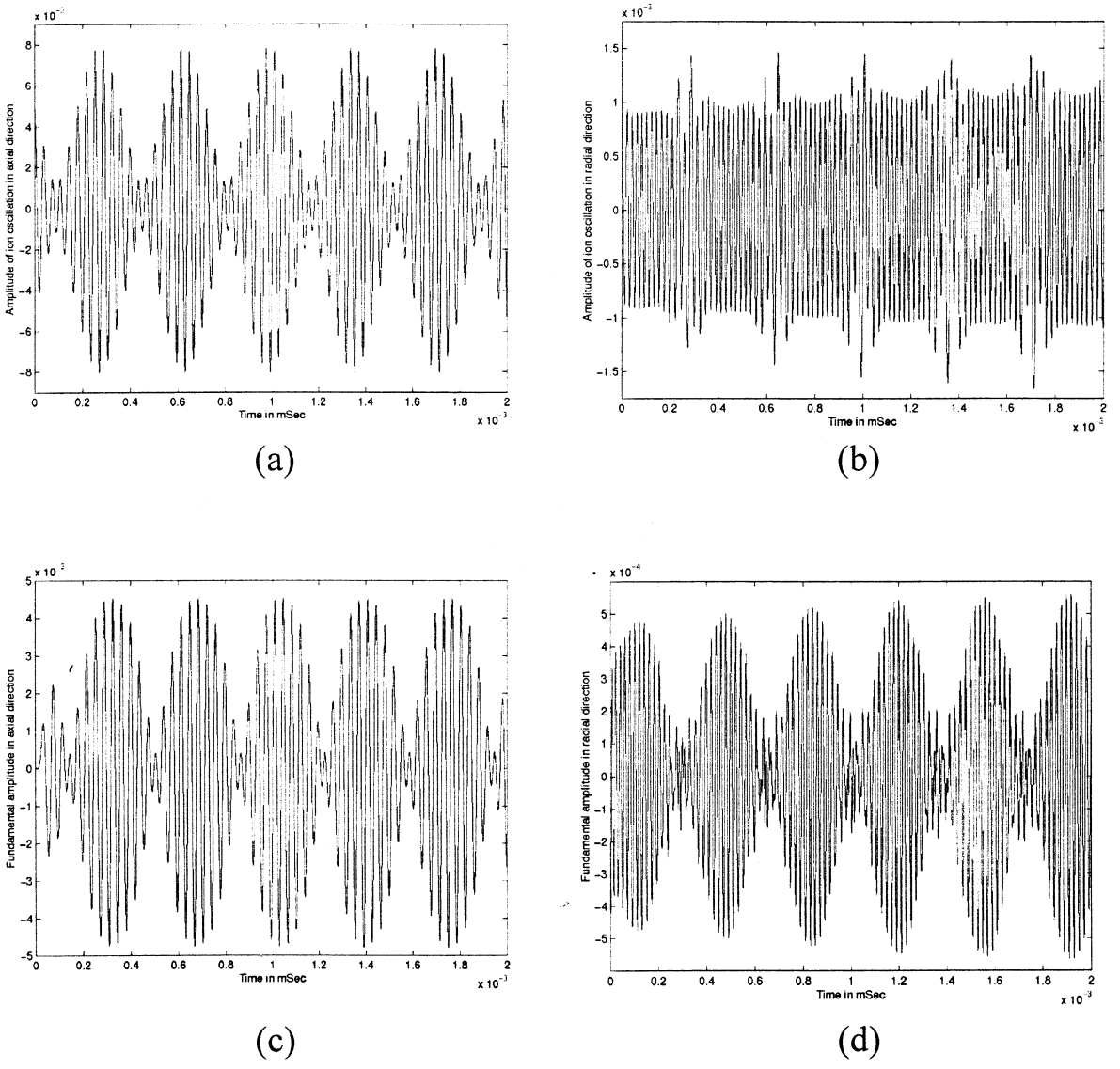

Fig. 1. (a) and (b) showing the time trace of axial and radial direction, respectively; (c) and (d) showing the fundamental secular frequency component filtered out from the trajectories of the ion motion in axial and radial direction, respectively.

Here $\in$ is a small dimensionless parameter and is introduced as a book keeping device, which will be set to unity in the final solution [55]. The term σ_z quantitatively describes the nearness of the excitation frequency (ω_z) to the ideal axial secular frequency (ω_{0z}). When $\sigma_z = 0$, as in the case of linear systems with no damping or nonlinearity, the amplitude of oscillations will be unbounded irrespective of how small the excitation is.

To obtain a uniformly valid approximate solution to this problem, it is necessary to order the external excitation and the nonlinearity in such way that their effect appears simultaneously in the same perturbation scheme [56]. Following Nayfeh and Mook [57], if we let $z = \in x$ and $r = \in y$, it is necessary to order excitation as $\in^3 F_s \cos(\omega_z t)$. This ordering scheme is valid for the primary resonance condition, that is when $\omega_z \cong \omega_{0z}$. With this order-

ing scheme, the equation of ion motion in the axial direction becomes

$$\frac{d^2x}{dt^2} + \omega_{0z}^2 x + \in\alpha_2 x^2 + \in^2 \alpha_3 x^3 - \in^2 \alpha_4 x y^2 = -\in^2 F_s \cos(\omega_z t) \quad (30)$$

Perturbation techniques assume that an approximate solution of the amplitude of the nonlinear equation can be written as an expansion that is valid for motions with small but finite amplitudes. In the Lindstedt–Poincare method, the variable chosen for the expansion is a single variable, namely independent time ($\tau = \omega t$). In multiple scales method, however, the expansion is generally written as a function of multiple independent variables, or scales, as follows [56]

$$x = \in x_1(T_0, T_1.T_2. \ldots) + \in^2 x_2(T_0, T_1.T_2. \ldots) + \in^3 x_3(T_0, T_1.T_2. \ldots) + \ldots \quad (31)$$

where the multiple independent variables have the form

$$T_n = \in^n t \quad \text{for } n = 0,1,2,\ldots \quad (32)$$

The number of independent time scales to be considered in a particular problem is a function of the order to which the expansion is desired and thus, in our case, where we compute up to $O(\in^3)$, we will require T_0, T_1, and T_2. Introducing Eqs. (29), (31), and (32) into Eq (30), and equating the coefficients of $\in$, $\in^2$, and $\in^3$ to zero, we obtain a series of partial derivatives as

$$D_0^2 x_1 + \omega_{0z}^2 x_1 = 0 \quad (33)$$

$$D_0^2 x_2 + \omega_{0z}^2 x_2 = -2D_0 D_1 x_1 - \alpha_2 x_1^2 \quad (34)$$

$$D_0^2 x_3 + \omega_{0z}^2 x_3 = -D_1^2 x_1 - 2D_0 D_2 x_1 - 2D_0 D_1 x_2 - 2\alpha_2 x_1 x_2 - \alpha_3 x_1^3 + \alpha_4 x_1 y_1^2 + F_s \cos(\omega_{0z} T_0 + \sigma_z T_2) \quad (35)$$

where $D_n = \partial/\partial T_n$. Eqs. (33) and (34) can be solved for getting x_2 by assuming a general solution to the Eq. (33) as

$$x_1 = A(T_1,T_2)\exp(i\omega_{0z}T_0) + \bar{A}(T_1,T_2)\exp(-i\omega_{0z}T_0) \quad (36)$$

where A is an unknown complex function, with $\bar{A}$ being the complex conjugate. Elimination of the secular term (i.e. the term whose amplitude increases with time) in any particular solution of Eq. (34) requires A to be independent of T_1. Similarly, in order to solve for x_3 from Eq. (35), x_1 and x_2 are substituted along with the assumption

$$y_1 = B(T_1,T_2)\exp(i\omega_{0r}T_0) + \bar{B}(T_1,T_2)\exp(-i\omega_{0r}T_0) \quad (37)$$

where y_1 is a general solution to equation of ion motion in radial direction, and B is an unknown complex function, with $\bar{B}$ being the complex conjugate. In Eq. (35), which is a partial differential equation with respect to T_2, it has been found convenient to write A and B in the polar form as

$$A = \frac{1}{2}a \exp(i\Phi_x) \quad (38)$$

$$B = \frac{1}{2}b \exp(i\Phi_y) \quad (39)$$

where a, b, Φ_x and Φ_y are real functions of T_2 and Φ_x and Φ_y represent the phase in the axial and radial direction respectively. Substituting Eq. (38) into Eq. (36) and substituting that result in Eq. (31) and setting $\in = 1$, we can see that a is the amplitude of ion oscillation in the axial direction. Similarly, while computing the perturbed frequency in the r direction, it turns out that b represents the amplitude of ion oscillation in the radial direction. Substituting x_1, x_2, y_1, A and B into Eq. (35) and separating the real and imaginary parts, we obtain

$$a' = \frac{f}{2\omega_{0z}a}\sin\gamma \quad (40)$$

$$\Phi_x' = \frac{9\alpha_3\omega_{0z}^2 T_\alpha - 10\alpha_2^2}{24\omega_{0z}^3} a^2 - \frac{\alpha_4}{4\omega_{0z}} b^2 - \frac{f}{2\omega_{0z}a}\cos\gamma \quad (41)$$

where

$$\gamma = \sigma_z T_2 - \Phi_x \tag{42}$$

and the primes denote the derivatives with respect to T_2. Differentiating Eq. (42) with respect to T_2 and substituting Φ_x' from Eq. (41), we get

$$\gamma = \sigma_2 - \frac{9\alpha_3\omega_2^{0z} - 10\alpha_2^2}{24\omega_{0z}^3}a^2 + \frac{\alpha_4}{4\omega_{0z}}b^2 + \frac{f}{2\omega_{0z}a}\cos\gamma \tag{43}$$

In order to obtain the frequency response relation that relates amplitude to the detuning parameter σ_z for ion motion in the axial direction, we need to locate the singular points. Singular points are those points at which amplitude and phase remain constant and corresponds to the steady state condition of the system. These points indicate whether the amplitude will decay or grow on introducing a small nonlinearity. Such singular points are obtained by equating $a' = \gamma' = 0$ in Eqs. (40) and (43).

Applying this steady state condition and squaring and adding Eqs. (40) and (43), we get the following frequency response relation

$$\sigma_z = \frac{9\alpha_3\omega_{0z}^2 - 10\alpha_2^2}{24\omega_{0z}^3}a^2 - \frac{\alpha_4}{4\omega_{0z}}b^2 + \frac{f}{2\omega_{0z}a} \tag{44}$$

The shifted frequency ω_z can now be calculated by substituting Eq. (44) in Eq. (29) and setting $\in = 1$ in Eq. (29). This yields

$$\omega_z = \omega_{0z}\left(1 + \frac{9\alpha_3\omega_{0z}^2 - 10\alpha_2^2}{24\omega_{0z}^4}a^2 - \frac{\alpha_4}{4\omega_{0z}^2}b^2 + \frac{f}{2\omega_{0z}^2a}\right) \tag{45}$$

Similarly, in the r direction, where there is no force term, the perturbation in radial secular frequency will be

$$\omega_r = \omega_{0r}\left(1 - \frac{3\alpha_5}{8\omega_{0r}^2}b^2 - \frac{\alpha_6}{4\omega_{0r}^2}a^2\right) \tag{46}$$

Eq. (45) indicates the dependence of the axial ion secular frequency on geometric aberration, excitation amplitude, and coupling. The second term inside the bracket expresses the magnitude of the perturbation due to geometric aberration. The third term contains the parameter α_4 that incorporates geometric aberration due to hexapole and octopole superposition and the radial amplitude's effect on axial secular frequency perturbation. The last term is related to the perturbation in secular frequency due to amplitude of external excitation. Similarly Eq. (46) shows the dependence of the radial ion secular frequency on geometric aberration and coupling. The second term inside the bracket expresses the magnitude of the perturbation due to geometric aberration. The third term contains the parameter α_6 that incorporates geometric aberration due to octopole superposition and the axial amplitude's effect on radial secular frequency.

6. Results and discussions

In the development of equations of ion motion in axial and radial directions, we have had to average the motion over the period of rf drive. This limits the applicability of the results presented in this paper to values of $q_u < 0.4$. Below this value of q_u, the frequencies obtained by Dehmelt approximations and that obtained by computing β_u using the continuous fraction [1,44] are in agreement to within 3%. Fig. 2 identifies the region in the Mathieu stability plot where a and q values can be used to compute secular frequencies within this percentage of error. A variety of secular frequency ratios can be obtained in this region.

With a view to understanding the nature of coupled oscillations between the axial and the radial secular motions, we first focused on numerical simulations with no external excitation. This was followed by numerical simulation of a mass spectrometrically relevant circumstance, that is, when an external excitation was applied as in resonance excitation experiments. All simulations were performed on an ion of 300 Th in a Paul trap having a 7 mm radius ring

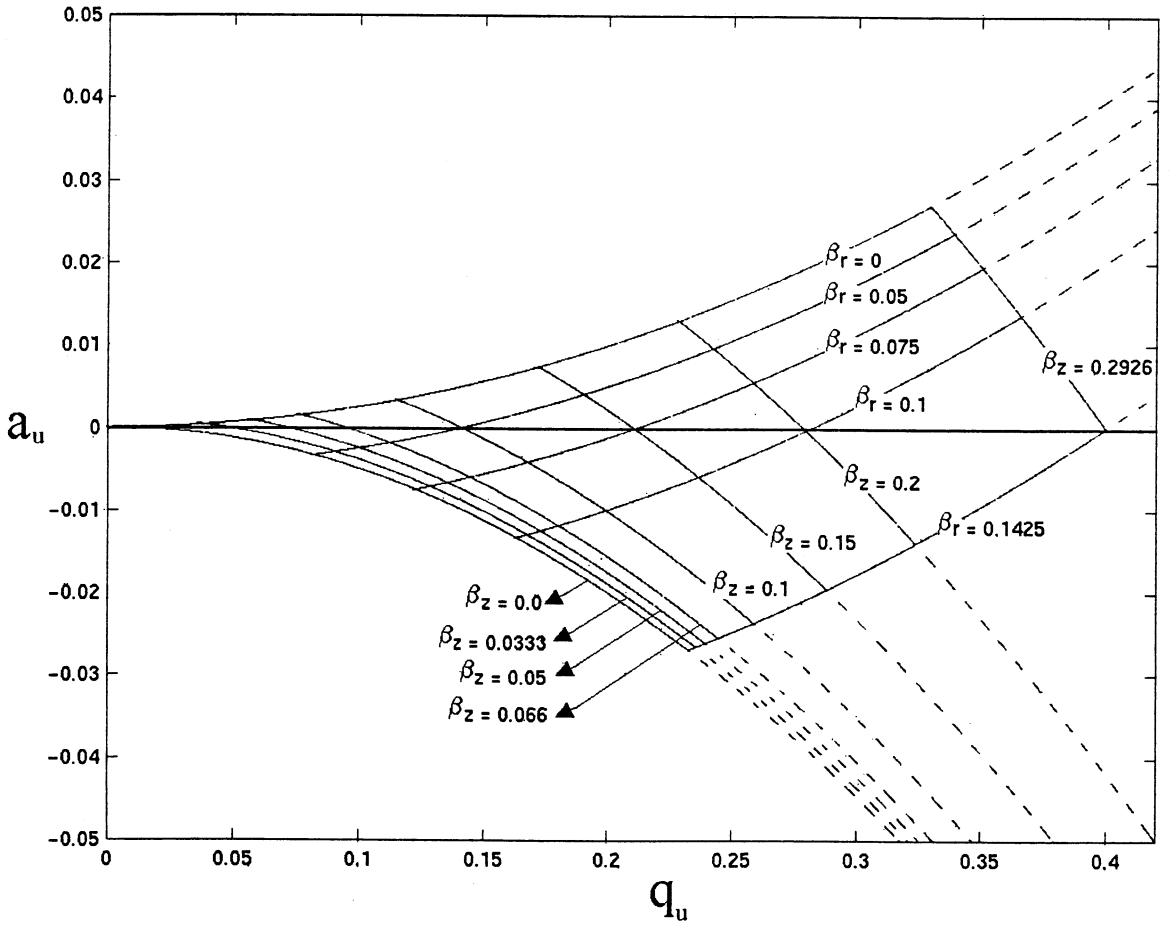

Fig. 2. Region of Mathieu stability plot considered in the present computations.

electrode and assuming $r_0^2 = 2z_0^2$. The *rf* voltage was fixed at $259.6V_{0-p}$ a frequency of 1 MHz and dc voltage has been kept at 9.3 V and 34 mV to obtain a β_z/β_r ratios of 0.5 and 2 respectively. The hexapole and octopole nonlinearity was varied between 0 to 2.5% and the applied external excitation potential was from 0 to 100 mV_{0-p} in the numerical simulations of ion trajectories. The initial position of the ions was kept at $z = 5e\text{-}3m$ and $r = 1e\text{-}3m$ and the initial velocity assumed to be zero in all the simulations. In order to study the effect of the coefficients of the cross terms in the equations of motion in determining the extent of coupling, we considered two frequency ratios $\omega_{0z}/\omega_{0r} = 1/2$ and 2. The variation of these ratios changes the magnitude of the coefficients of the cross terms in the equation of motion in both *z* and *r* directions. It is to be noted that these are ratios of the ideal secular frequencies in the axial and the radial directions and not of the perturbed secular frequencies. Indeed, the ratio of the corresponding perturbed frequencies will not have this integer relationship.

The frequencies indexed in all the plots correspond to the perturbed axial and radial secular frequencies. In all frequency spectra, the amplitudes of frequency components have been considerably enlarged for the sake of clarity. The typical amplitude of the fundamental secular frequencies is in the region of 10^{-3} m as is evident from the ion trajectory plots, whereas the

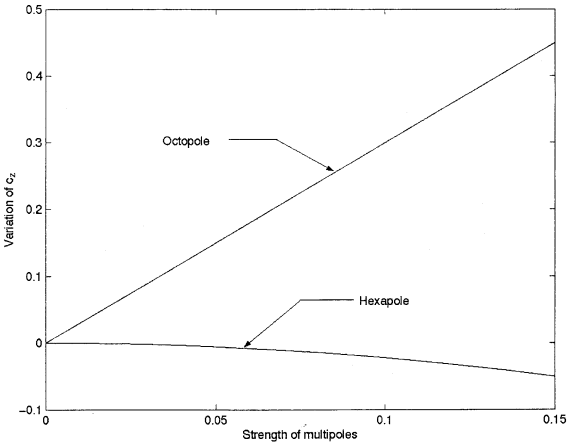

Fig. 3. Variation of c_z with hexapole and octopole superposition.

magnitudes of the coupled frequencies are in the region of 10^{-7} m.

For a specific operating point, c_z and c_r [in Eqs. (20) and (21)] represent the contribution of field nonlinearity to the coefficient of the cross terms. Fig. 3 shows the dependence of c_z on hexapole and octopole concentration, and Fig. 4 the dependence of c_r on octopole superposition in the absence of external excitation, that is when $V_s = 0$. Hexapole nonlinearity does not affect the magnitude of c_z significantly and since it appears as a quadratic term, the sign of this superposition is unimportant. However, as these figures show, the magnitude of c_z and c_r increases

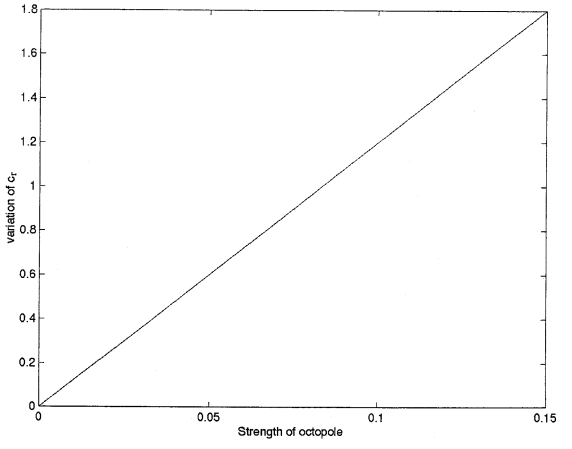

Fig. 4. Variation of c_r with octopole superposition.

linearly with increase in octopole superposition. Although these coefficients are of the same order of magnitude in both directions, it will be seen that the overall contribution of the coefficient of the cross terms in the equations of motion is determined by the geometry (r_0) as well as the operating point (which determines ω_{0z} and ω_{0r}) of the trap.

Trajectories of axial and radial motion in the absence of external excitation are shown in Figs. 5 and 6 for values of $\beta_z/\beta_r = 1/2$ and $\beta_z/\beta_r = 2$, respectively. The dc potential was kept at 9.3 V and 34 mV to get $\beta_z/\beta_r = 1/2$ and 2, respectively and the hexapole superposition was set at 1% and octopole at 2.5%. Figs. 5(a) and 6(a), represent the fundamental frequency component in the axial direction, and Figs. 5(b) and 6(b) the same in the radial direction. Figs. 5(c), 5(d), and 6(c), 6(d) represents the frequency spectrum obtained by Fourier transform of the corresponding unfiltered ion trajectories.

The behavior of coupled ion motion at different operating points was analyzed by taking the coefficients of cross terms in the equations of ion motion, i.e. α_4 and α_6 in z and r direction, respectively, to represent the coupling strength. When $\beta_z/\beta_r = 1/2$ (that is when the ratio of the ideal secular frequencies $\omega_{0z}/\omega_{0r} = 1/2$), the ratio of the coefficients of the cross terms in the equations of ion motion (α_4/α_6) is 0.0623. The coupling strength in the r direction is sixteen times stronger than that in the z direction. This gives rise to the appearance of axial secular frequency components in the radial direction in addition to the radial secular frequency and its harmonics. In contrast, since the coupling strength in the axial direction, is lower, the frequency spectrum of this direction consists only of secular frequency and its harmonics.

When $\beta_z/\beta_r = 2$, i.e. when $\omega_{0z}/\omega_{0r} = 2$, the ratio of the coefficients of the cross terms in the equation of motion (α_4/α_6) is 0.997 indicating that coupling strength in both directions is almost equal. The filtered ion trajectories and the corresponding frequency spectrum of the unfiltered time trace are shown in Fig. 6. Because of the relative increase in coupling strength in the z direction (in comparison with the case when $\beta_z/\beta_r = 1/2$), the frequency spectrum in axial direction acquires radial secular

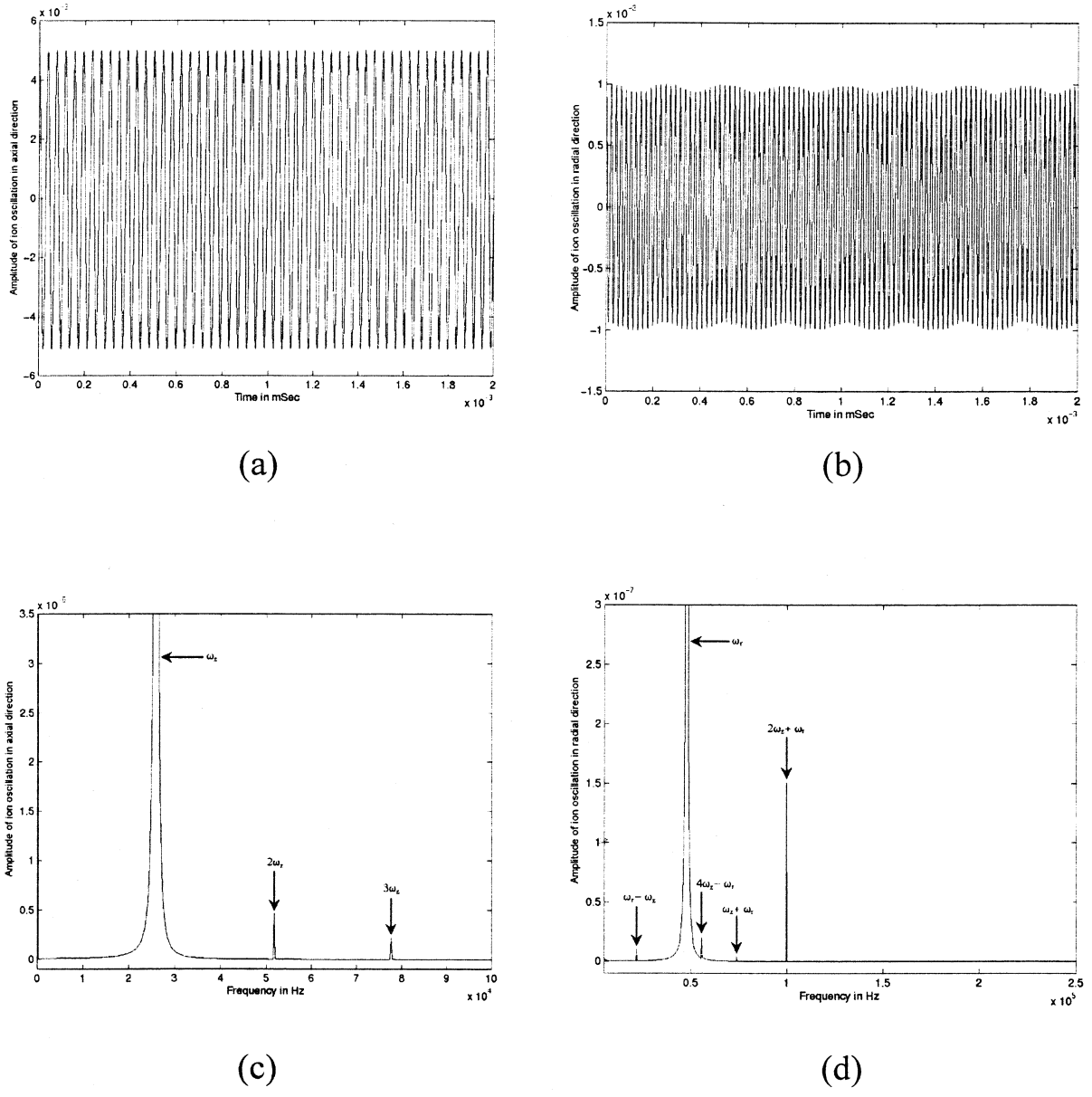

Fig. 5. (a) and (b) show the fundamental frequency components in axial and radial directions, respectively; (c) and (d) show the respective Fourier spectrum of ion trajectories when $\beta_z/\beta_r = 1/2$ and when there is no supplementary excitation.

frequency and its harmonics. Some of the prominent frequencies that we have indexed are $\omega_z - 2\omega_r$, ω_z, $\omega_z + 2\omega_r$, $2\omega_z$, and $3\omega_z$. The appearance of peaks such as $\omega_z \pm 2\omega_r$ indicates a coupling between the ion secular motion in the axial and radial directions. Since the ratio of the coupling strength in both directions is close to unity, the frequency spectrum of unfiltered radial motion also indicates the appearance of axial frequency components. Some of these indexed peaks are $\omega_z - \omega_r$, $2\omega_z - \omega_r$, and $2\omega_z + \omega_r$.

Let us next turn to the situation when an external supplementary voltage is applied to the end cap

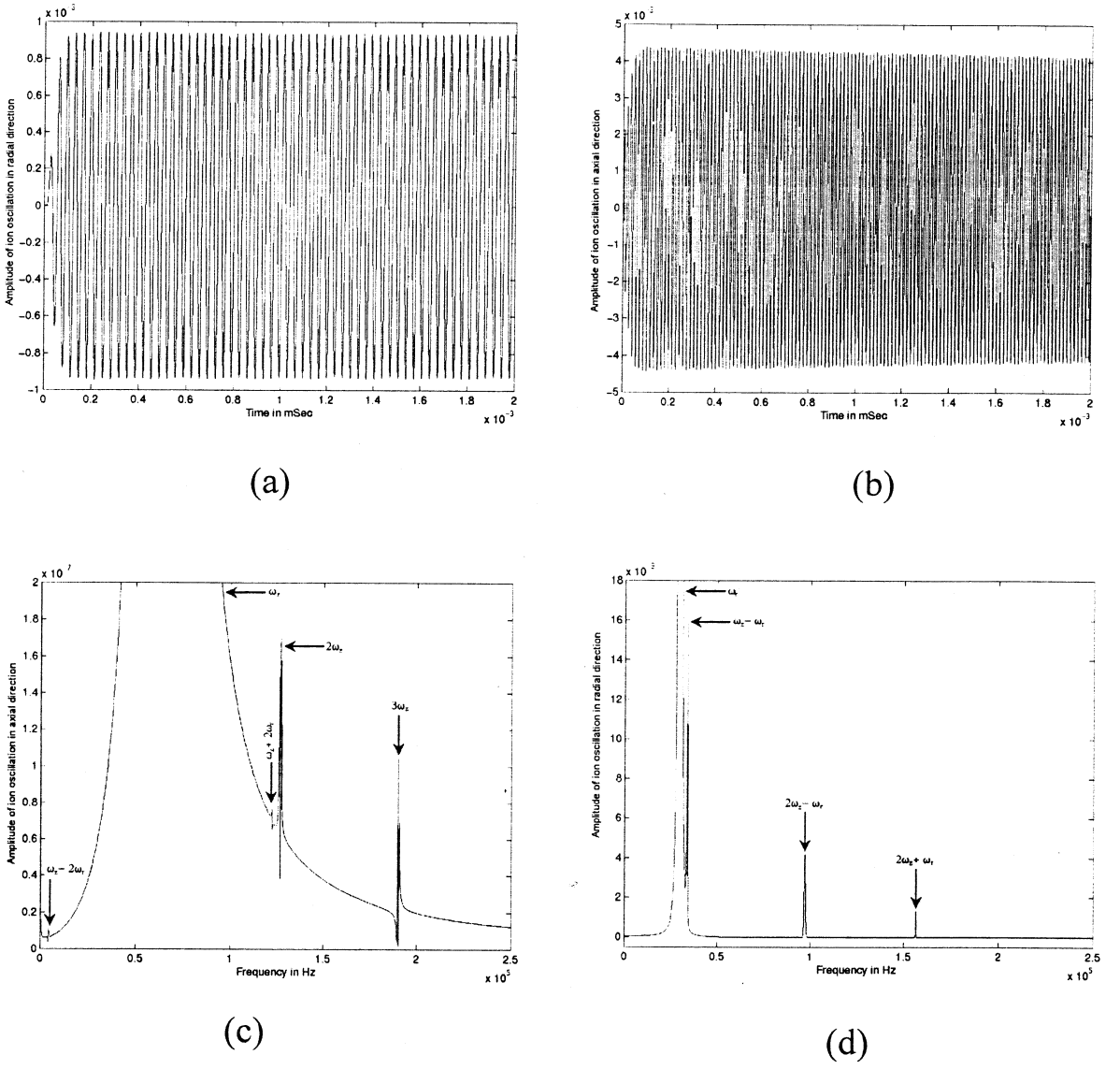

Fig. 6. (a) and (b) show the fundamental frequency components in axial and radial directions, respectively; (c) and (d) show the respective Fourier spectrum of ion trajectories when $\beta_z/\beta_r = 2$ and when there is no supplementary excitation.

electrode. The response of the system to the inclusion of the force term in axial secular motion is shown in Figs. 7 and 8 where $\beta_z/\beta_r = 1/2$, and $\beta_z/\beta_r = 2$, respectively. Here the simulation conditions are the same as those of Fig. 5 and 6 except that an additional external excitation potential of 100 mV is applied to the end cap electrodes. In the first instance (Fig. 7) where ω_{0r} is larger than ω_{0z}, the axial secular frequency spectrum [Fig. 7(c)] continues to be simple with appearance of only the axial secular frequency and its harmonics. This is similar to the frequency spectrum when $V_s = 0$ [Fig. 5(c)]. However, with the application of external excitation the radial frequency spectrum (Fig. 7(d)) acquires many more frequency components. Some of the prominent peaks include $2\omega_z - \omega_r$, $4\omega_z - 2\omega_r$, $6\omega_z - 2\omega_r$ in addition to several others that have not been indexed.

Fig. 8 has been plotted for the condition when

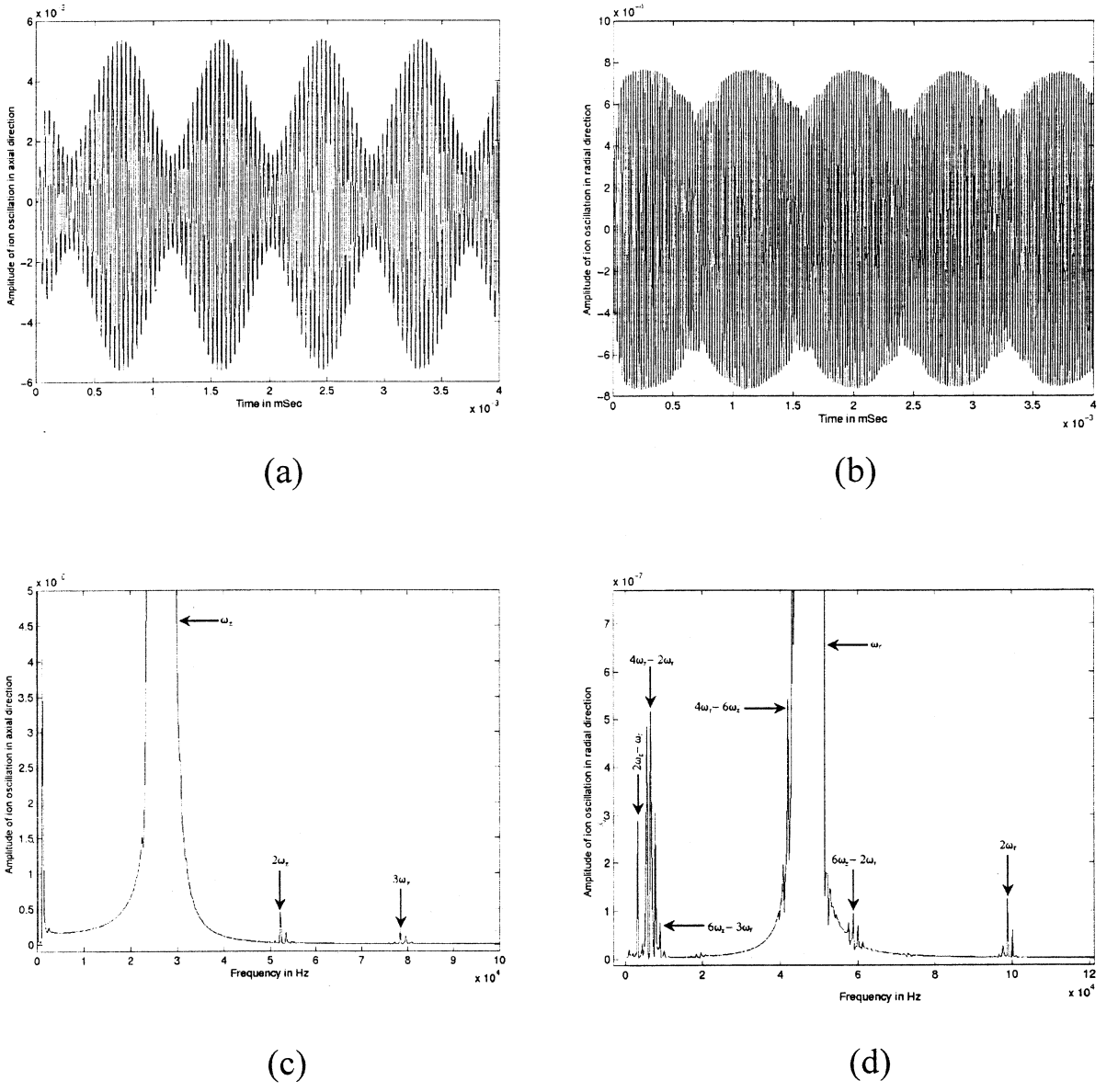

Fig. 7. (a) and (b) show the fundamental frequency components in axial and radial directions, respectively; (c) and (d) show the respective Fourier spectrum of ion trajectories when $\beta_z/\beta_r = 1/2$ and when there is a supplementary excitation of 100 mV.

β_z/β_r $(= \omega_{0z}/\omega_{0r}) = 2$. Since the axial secular frequency is larger than the radial secular frequency, it may be recalled that the ratio of the coupling strength in the axial and radial direction is close to unity in our computations. As the coupling strength of axial motion increases, radial frequencies begin to appear in the frequency spectrum of unfiltered axial motion. Some of the prominent peaks include $\omega_z - \omega_r$, $\omega_z + 2\omega_r$ (Fig. 8(c)). Similarly, as the coupling strength in the radial direction decreases the frequency spectrum displays a reduced number of frequencies. A few prominent peaks include $\omega_z/2$, $2\omega_z - \omega_r$, and $2\omega_z + \omega_r$ [Fig. 8(d)].

In physical systems in which frequencies of two

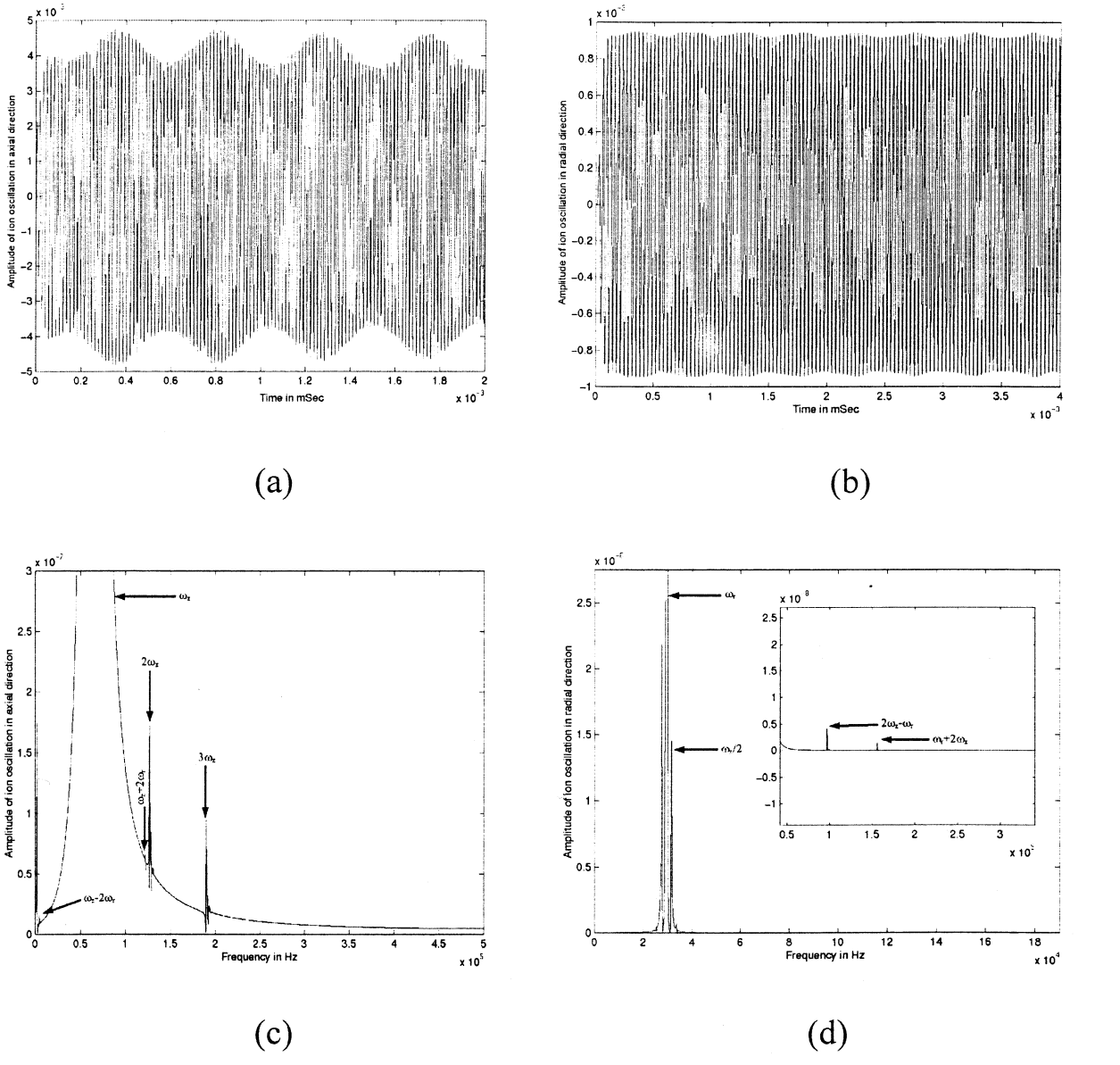

Fig. 8. (a) and (b) show the fundamental frequency components in axial and radial directions, respectively; (c) and (d) show the respective Fourier spectrum of ion trajectories when $\beta_z/\beta_r = 2$ and when there is a supplementary excitation of 100 mV.

coupled oscillating modes do not form a harmonic series, mixing of frequencies occurs to produce a resultant which are combinations of the frequencies originally present [58]. The frequencies that are of interest in our simulations are the perturbed axial and radial secular frequencies, the frequency of the external excitation, and the harmonics of the secular frequencies. In addition, it is known that in nonlinear systems, harmonics of the secular frequencies will exist, the amplitude of these harmonics being determined by the specific nonlinear conditions of the system [56,59,60]. Such harmonic frequencies have also been observed in cylindrical traps in the image current measurements made by Cooks and coworkers

[20,39]. Consequently, harmonic frequencies will also participate in frequency mixing, resulting in a variety of frequencies in the frequency spectrum. The results of our simulations with and without external excitation indicate such a behavior. In the absence of external excitation, the components of the frequency spectrum are essentially combination frequencies of axial and radial motions and their harmonics. In the presence of external excitation, the components of the frequency spectrum increase in number because of the mixing of a larger number of harmonics in the axial and radial directions.

In the context of mixing, an interesting aspect of ion motion is seen in Figs. 7 and 8 with the appearance of a distinct beat structure in the axial and the radial motions that are 180° out of phase. In mechanical systems such beat patterns are attributed to amplitude and phase modulation caused by the external excitation [45]. In the simulation of ion motion in the axial direction, the frequency of external excitation was fixed as the ideal secular frequency of the system. This frequency was based on the β value computed from the continuous fraction expression and inserted into Eq. (20). The program internally computes the perturbed frequency during the simulations. It turns out that the frequency of the convolute of fundamental component in the axial direction is the difference between the ideal secular frequency and the perturbed secular frequency and corresponds to the difference between Eq. (45) and ω_{0z}, and can be represented by

$$\Delta\omega_z = \left(\frac{9\alpha_3\omega_{0z}^2 - 10\alpha_2^2}{24\omega_{0z}^3}\alpha^2 + \frac{\alpha_4}{4\omega_{0z}}b^2 + \frac{f}{2\omega_{0z}a}\right) \tag{47}$$

The beat structure in the radial direction has the same frequency as this, and the amplitude modulation of this beat frequency in the radial direction depends primarily on the coupling strength in the radial direction. In Fig. 7(b), in which the coupling strength in the radial direction is stronger, the amplitude modulation of the radial direction is significantly larger than that in Fig. 8(b) for the same excitation amplitude (V_s = 100 mV). This difference holds when we compare this with the amplitude modulation shown in Fig. 1 in which the trajectories have been computed for V_s = 300 mV.

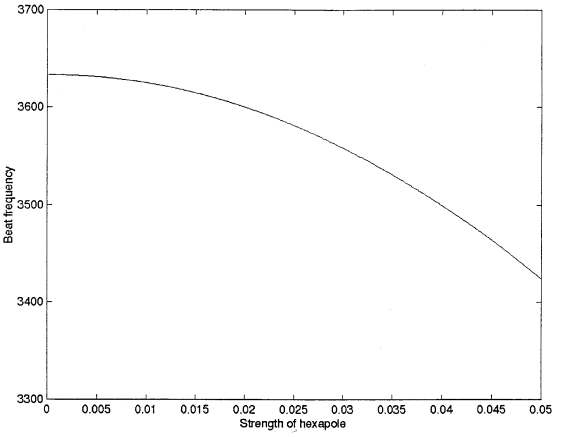

Fig. 9. Variation of beat frequency with hexapole superposition.

The variation of the beat frequency with nonlinearity is shown in Figs. 9, 10, and 11. While the number of beats decreases with increase in the hexapole superposition (Fig. 9), the number of beats increases with both octopole superposition (Fig. 10) and amplitude of the external excitation term (Fig. 11). Hexapole superposition does not change the beat frequency significantly. In contrast, octopole superposition changes the beat frequency to a larger extent. For a given trap, larger amplitudes of external exci-

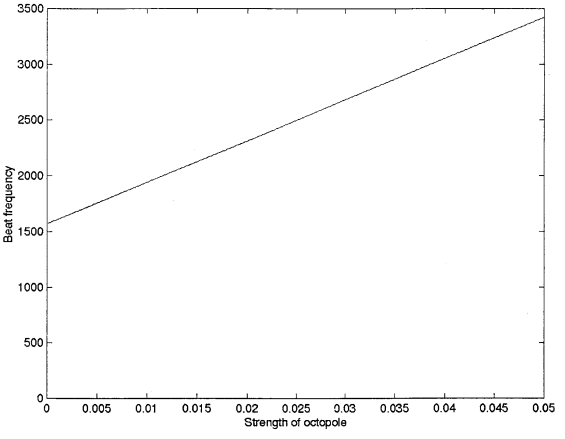

Fig. 10. Variation of beat frequency with octopole superposition.

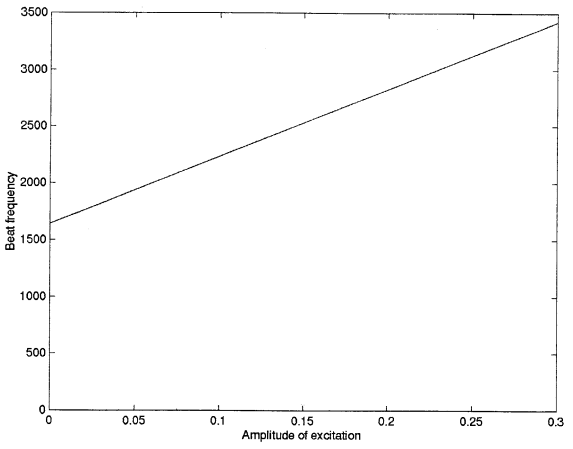

Fig. 11. Variation of beat frequency with excitation potential.

tation will also result in increasing the beat frequency since this amplitude contributes to frequency perturbation.

One last observation that needs to be reported has to do with the frequency ratios used in our computations. For contrasting frequency spectra associated with coupled oscillations, we have used two ratios, namely $\omega_{0z}/\omega_{0r} = 1/2$ and $\omega_{0z}/\omega_{0r} = 2$. While these ratios correspond to the ideal secular frequencies, a look at Eqs. (45) and (46) indicates that the perturbed frequency, that is the secular frequency of the ions in the presence of nonlinearities, have a ratio different from 1/2 and 2. For a given set of nonlinearities, frequency perturbation in axial and radial direction will change in opposite directions. For instance, an increase in octopole superposition increases the axial secular frequency, but decreases the radial secular frequency. In the specific simulations we have reported in Fig. 7, when the $\omega_{0z}/\omega_{0r} = 1/2$, the ratio of the corresponding perturbed frequency, $\omega_z/\omega_r = 0.55$. Similarly, when $\omega_{0z}/\omega_{0r} = 2$, the ω_z/ω_r is calculated as 2.17. What our simulation then suggests is that in practical traps, even when the frequency ratio does not bear an integer relationship, the coupling will continue to exist and the extent of coupling will be determined by the degree of nonlinearity within the trap.

7. Conclusions

The motivation behind this paper was to understand the role of some factors that influence coupled axial and radial oscillations and cause perturbation of ion secular frequencies in nonlinear Paul trap mass spectrometers. In our simulations, we have examined the role of geometric aberration and amplitude of the external excitation for different values of β_z/β_r associated with an ion.

Our study is relevant to mass spectrometry experiments that estimate ion secular frequencies for mass assignment. This study suggests that two important factors that arise due to the presence of nonlinear fields in practical traps needs to be considered for mass assignment. The first is that nonlinear fields within the trap will perturb ion secular frequencies. This perturbation is caused not only by geometric aberrations but also by the presence of external excitation. A large magnitude external excitation causes larger frequency shifts. This is especially important in broadband image current detection that require large amplitude external excitation to obtain acceptable signal to noise ratios [20]. The second consequence of nonlinear fields is the appearance of harmonics and coupled oscillations. In nondestructive detection techniques for measurement of ion secular frequencies, the presence of harmonics and coupled oscillations will lead to the appearance of phantom peaks in the frequency spectrum. The magnitude of the phantom peaks in our simulations was seen to be several orders lower than the base peak magnitude. Their existence, however, may prove pertinent under other experimental conditions. Further, the number of phantom peaks associated with a specific mass was seen to depend on the β_z/β_r value associated with it.

Acknowledgements

The authors would like to thank Prof. Mrinal K. Ghosh and Prof. A. K. Nandakumaran, both of Department of Mathematics, and Prof. R. M. Vasu, Department of Instrumentation, for their role in several discussions. The authors are grateful to Prof. Thomas Chacko, Foreign Language Section, for sparing his time to copyedit the manuscript.

References

[1] R.E. March, R.J. Hughes, Quadrupole Storage Mass Spectrometry, Wiley-Interscience, New York, 1989.
[2] R.D. Knight, Int. J. Mass Spectrom. Ion Phys. 51 (1983) 127.
[3] P.H. Dawson, Quadrupole Mass Spectrometry and it's Application, Elsevier, Amsterdam, 1976.
[4] R.F. Wuerker, H. Shelton, R.V. Langmuir, J.Appl.Phys. 30 (1959) 342.
[5] M. Abromowitz, I.A. Stegun, Handbook of Mathematical Functions, Dover Publications Inc., New York, 1970.
[6] F.G. Major, H.G. Dehmelt, Phys. Rev. 170 (1968) 91.
[7] J. Louris, J. Schwartz, G. Stanfford, J. Syka, D. Taylor, Proceedings of the 40th ASMS Conference on Mass Spectrometry Allied Topics, Washington, DC, 1992, p.1003.
[8] K. Sugiyama, J. Yoda, Appl. Phys. B 51 (1990) 146.
[9] F. Vedel, M. Vedel, in R.E. March, J.F.J. Todd (Eds.), Practical Aspects of Ion Trap Mass Spectrometry, CRC, New York, 1995, Vol. 1, Chap. 8, p.346.
[10] K.A. Cox, C.D. Cleven, R.G. Cooks, Int. J. Mass Spectrom. Ion Processes 144 (1995) 47.
[11] X. Luo, X. Zhu, K. Gao, J. Li, M. Yan, L. Shi, J. Xu, Appl. Phys. B 62 (1996) 421.
[12] J.F.J. Todd, R.M. Waldren, D.A. Freer, R.B. Turner, Int. J. Mass Spectrom. Ion Phys. 35 (1980) 107.
[13] R.L. Alfred, F.A. Londry, R.E. March, Int. J. Mass Spectrom. Ion Processes, 125 (1993) 171.
[14] D.E. Goeringer, R.I. Crutcher, S.A. McLuckey, Anal. Chem. 67 (1995) 4164.
[15] J.D. Williams, K.A. Cox, R.G. Cooks, S.A. McLuckey, K.J. Hart, D.E. Goeringer, Anal. Chem. 66 (1994) 725.
[16] F. Vedel, M. Vedel, R.E. March, Int. J. Mass Spectrom. Ion Processes 99 (1990) 125.
[17] R.K Julian, R.G. Cooks, Anal. Chem. 65 (1993) 1827.
[18] J. Franzen, R.H. Gabling, M. Schubert, Y. Wang, in R.E. March, J.F.J. Todd (Eds.), Practical Aspects of Ion Trap Mass Spectrometry, CRC, New York, 1995, Vol. 1, Chap. 3 pp.49.
[19] J.E. Fulford, D.-N. Hoa, R.J. Hughes, R.E. March, R.F. Bonner, G.J. Wong, J. Vac. Sci. Technol. 17 (1980) 829.
[20] M. Nappi, V. Frankevich, M.Soni, R.G. Cooks, Int. J. Mass Spectrom. Ion Processes 177 (1998) 91.
[21] X.Z. Chu, M. Holzki, R. Alheit, G. Werth, Int. J. Mass Spectrom. Ion. Processes 173 (1998) 107.
[22] F. Vedel, M. Vedel, Phys. Rev. A 41 (1990) 2348.
[23] M. Vedel, J. Rocher, M. Knoop, F. Vedel, Appl. Phys. B 66 (1998) 191.
[24] Y. Wang, J. Franzen, K.P. Wanczek, Int. J. Mass Spectrom. Ion Processes 124 (1993) 125.
[25] A.A. Makarov, Anal. Chem. 68 (1996) 4257.
[26] J.J. Stoker, Nonlinear Vibrations, Interscience Publishers, New York, 1950.
[27] N.W. McLachlan, Ordinary Nonlinear Differential Equations in Engineering and Physical Sciences, Oxford University, London, 1958.
[28] S. Sevugarajan, A.G. Menon, Int. J. Mass Spectrom. 189 (1999) 53.
[29] S. Sevugarajan, A.G. Menon, Int. J. Mass Spectrom. 197 (2000) 263.
[30] F.A. Londry, R.L. Alfred, R.E. March, J. Am. Soc. Mass. Spectrom. 4 (1993) 687.
[31] R.E. March, A.W. McMahon, F.A. Londry, R.L. Alfred, J.F.J. Todd, F. Vedel, Int. J. Mass Spectrom. Ion Processes 95 (1989) 119.
[32] R.E. March, A.W. McMahon, E.T. Allinson, F.A. Londry, R.L. Alfred, J.F.J. Todd, F. Vedel, Int. J. Mass Spectrom. Ion Processes 99 (1990) 109.
[33] H.A. Bui, R.G. Cooks, J. Mass Spectrom. 33 (1998) 297.
[34] D.J. Wineland, W.M. Itano, R.S. Van Dyck, Jr, in D. Bates, B. Bederson (Eds.), Advances in atomic and molecular physics, Vol. 19, Academic, New York, 1983.
[35] D. Engelke, C.H.R. Tamm, Europhys. Lett. 33 (1996) 347.
[36] M. Roberts, P. Taylor, G.P. Barwood, P. Gill, H.A. Klein, W.R.C. Rowley, Phys. Rev. Lett. 78 (1997) 1876.
[37] P. Taylor, M. Roberts, G.P. Barwood, P. Gill, Opt. Lett. 23 (1998) 298.
[38] R.E. March, J.F.J. Todd (Eds.), Practical Aspects of Ion Trap Mass Spectrometry, Vol. III, CRC, New York, 1995.
[39] E.R. Badman, J.M. Wells, H.A. Bui, R.G. Cooks, Anal. Chem. 70 (1998) 3545.
[40] L.S. Brown, G. Gabrielse, Rev. Mod. Phys. 58 (1986) 233.
[41] E.C. Beaty, Phys. Rev. A 33 (1986) 3645.
[42] Y. Wang, J. Franzen, Int. J. Mass Spectrom. Ion Processes 132 (1994) 155.
[43] L.D. Landau, E.M. Lifshitz, Mechanics, 3rd Ed., Pergamon, U.K., 1976.
[44] R.E. March, F. A. Londry, in R.E. March, J.F.J. Todd (Eds.), Practical Aspects of Ion Trap Mass Spectrometry, CRC, New York, 1995, Vol. 1, Chap. 2, p. 25.
[45] A.H. Nayfeh, L.D. Zavodney, Trans. ASME. J. Appl. Mech. 55 (1988) 706.
[46] S.A. Nayfeh, A.H. Nayfeh, Int. J. Bifurcation Chaos Appl. Sci. Eng. 3 (1993) 417.
[47] A.H. Nayfeh, D.T. Mook, L.R. Marshall, J. Hydronautics 7 (1973) 145.
[48] G.J. Efstathiades, J. Sound Vib. 10 (1969) 81.
[49] T. Yamamoto, K. Yasuda, Bull. JSME 20 (1977) 168.
[50] T.S. Reynolds, E.H. Dowell, Int. J. Nonlinear Mech. 31 (1996) 941.
[51] W.Y. Tseng, J. Dugundji, Trans. ASME. J. Appl. Mech. 38 (1971) 467.
[52] W.M. Tien, N.S. Namachchivaya, A.K. Bajaj, Int. J. Nonlinear Mech. 29 (1994) 349.
[53] MATLAB Reference Guide, The Math Works, Inc., Boston, MA, 1992.
[54] A.H. Nayfeh, Perturbation Methods, Wiley-Interscience, New York, 1973.
[55] A.H. Nayfeh, Problems in Perturbation, Wiley-Interscience, New York, 1985.
[56] A.H. Nayfeh, D.T. Mook, Nonlinear Oscillations, Wiley-Interscience, New York, 1979.
[57] A.H. Nayfeh, J. Sound Vib. 92 (1984) 363.
[58] A.B. Pippard, The Physics of Vibrations, Cambridge University Press, Cambridge, 1989.
[59] J. Padovan, I. Zeid, Int. J. Nonlinear Mech. 16 (1981) 465.
[60] M.S. Sharma, A.P. Beena, B.N. Rao, J. Sound Vib. 180 (1995) 177.